View Article Online
DOI: 10.1039/D3CC02142D

COMMUNICATION

Brominated [20]silafulleranes: pushing the limits of steric loading

Marcel Bamberg,[a] Thomas Gasevic,[b] Michael Bolte,[a] Alexander Virovets,[a] Hans-Wolfram Lerner,[a] Stefan Grimme,[b] Markus Bursch[c] and Matthias Wagner[a]*

Received 00th January 20xx,
Accepted 00th January 20xx

DOI: 10.1039/x0xx00000x

Starting from the perhydrogenated silafullerane [nBu$_4$N][Cl@Si$_{20}$(SiH$_3$)$_{12}$H$_8$], treatment with BBr$_3$ leads to partially and exhaustively brominated clusters, [nBu$_4$N][Cl@Si$_{20}$(SiBr$_2$H)$_{12}$Br$_8$] (120 eq. BBr$_3$, room temperature, 30 min) and [nBu$_4$N][Cl@Si$_{20}$(SiBr$_3$)$_{12}$Br$_8$] (300 eq. BBr$_3$, 130 °C, 3 d). Perbromination is accompanied by a massively increased steric strain on the cluster surface, which explains why our approach achieves regioselective derivatization of the Si$_{32}$ framework when mild conditions are maintained. Partial Br/H exchange on [nBu$_4$N][Cl@Si$_{20}$(SiBr$_2$H)$_{12}$Br$_8$] (30 eq. iBu$_2$AlH, room temperature, 16 h) affords [nBu$_4$N][Cl@Si$_{20}$(SiH$_3$)$_{12}$Br$_8$].

The siladodecahedranes [nBu$_4$N][Cl@Si$_{20}$(SiR$_3$)$_{12}$R$_8$] ("silafulleranes"; Fig. 1)[1–8] are among the largest structurally authenticated oligosilanes and represent a new class of saturated silicon cages (along with, for example, silatetrahedranes,[9,10] silacubanes,[11,12] and silaadamantanes[13,14]). Together with the unsaturated siliconoids[15–18] and the completely ligand-free Zintl ions,[19–21] these form the trinity of molecular silicon clusters.[22] Each of the [Cl@Si$_{20}$(SiR$_3$)$_{12}$R$_8$]$^-$ entities consists of an Si$_{20}$ core that encapsulates a Cl$^-$ ion and is decorated with 12 SiR$_3$ groups and 8 R atoms in perfect T_h symmetry.[1,3] For future development, it would be desirable if the silafulleranes did not carry 44 of the same functional groups R, but at least two different types of substituents R and R' with largely orthogonal reactivity so that R and R' can be addressed individually. Considering that both

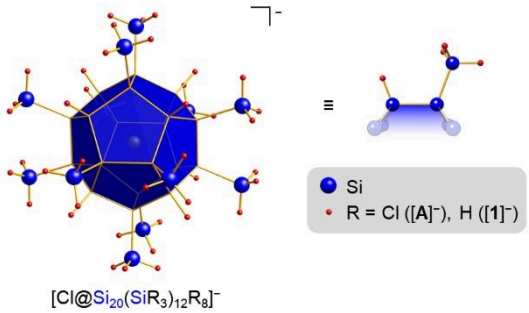

Fig. 1 Silafullerane anions [Cl@Si$_{20}$(SiR$_3$)$_{12}$R$_8$]$^-$ ([**A**]$^-$/[**1**]$^-$; R = Cl/H);[1,3] a representative fragment containing one Si–R and one Si–SiR$_3$ vertex is depicted separately.

the perhydrogenated silafullerane [nBu$_4$N][Cl@Si$_{20}$(SiH$_3$)$_{12}$H$_8$] ([nBu$_4$N][**1**])[3] and its perchlorinated analog [nBu$_4$N][Cl@Si$_{20}$(SiCl$_3$)$_{12}$Cl$_8$] ([nBu$_4$N][**A**])[1] exist and that SiH moieties provide highly diagnostic NMR handles, the most obvious choice would be R/R' = H/Cl. Indeed we have recently succeeded in the synthesis of the mixed H/Cl-silafullerane [nBu$_4$N][Cl@Si$_{20}$(SiH$_3$)$_{12}$Cl$_8$] ([nBu$_4$N][**B**]) by partial Cl/H exchange on [nBu$_4$N][**A**]. This approach was based on the higher reactivity of the sterically exposed silyl groups compared to the more protected core positions toward the H$^-$ donor iBu$_2$AlH.[3] However, a reverse synthesis strategy for partially halogenated silafulleranes, starting from [nBu$_4$N][**1**], also appears promising, since an increase in steric hindrance at the cluster surface as halogenation proceeds could keep some of the H substituents in place. Earlier quantum-chemical calculations have indicated that the perchlorinated framework of [**A**]$^-$ already probes the limits of steric bulk.[1] In bromination of [**1**]$^-$, the chance that a defined number of Si–H bonds will remain should therefore be even higher than in chlorination.

Herein, we report that this conceptual approach is indeed valid, as the treatment of [nBu$_4$N][**1**] with BBr$_3$ under varying conditions, combined with subsequent partial hydrogenation,

[a] *Institut für Anorganische und Analytische Chemie, Goethe-Universität Frankfurt am Main, Max-von-Laue-Straße 7, 60438 Frankfurt am Main (Germany). E-Mail: matthias.wagner@chemie.uni-frankfurt.de*
[b] *Mulliken Center for Theoretical Chemistry, Clausius-Institut für Physikalische und Theoretische Chemie, Rheinische Friedrich-Wilhelms-Universität Bonn, Beringstraße 4, 53115 Bonn (Germany).*
[c] *Max-Planck-Institut für Kohlenforschung, Kaiser-Wilhelm-Platz 1, 45470 Mülheim an der Ruhr (Germany).*
Electronic Supplementary Information (ESI) available: Experimental procedures, NMR, mass, and IR spectra, crystallographic data, and computational details. CCDC 2260148 and 2260149. See DOI: 10.1039/x0xx00000x

View Article Online
DOI: 10.1039/D3CC02142D

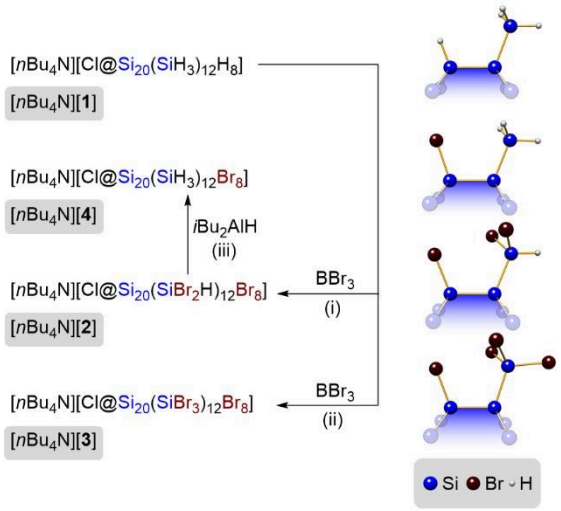

Scheme 1 Syntheses of the mixed H/Br-substituted silafulleranes [nBu$_4$N][**2**]–[nBu$_4$N][**4**] from [nBu$_4$N][**1**]. (i) 120 eq. BBr_3, *o*DFB, room temperature, 30 min, >90%; (ii) 300 eq. BBr_3, *o*DFB, 130 °C, 3 d, manually picked crystals; (iii) 30 eq. iBu$_2$AlH, *o*DFB/Et$_2$O, room temperature, 16 h, 35%. The substitution patterns are illustrated by representative cluster fragments containing one Si–R and one Si–SiR_3 vertex (R = H, Br).

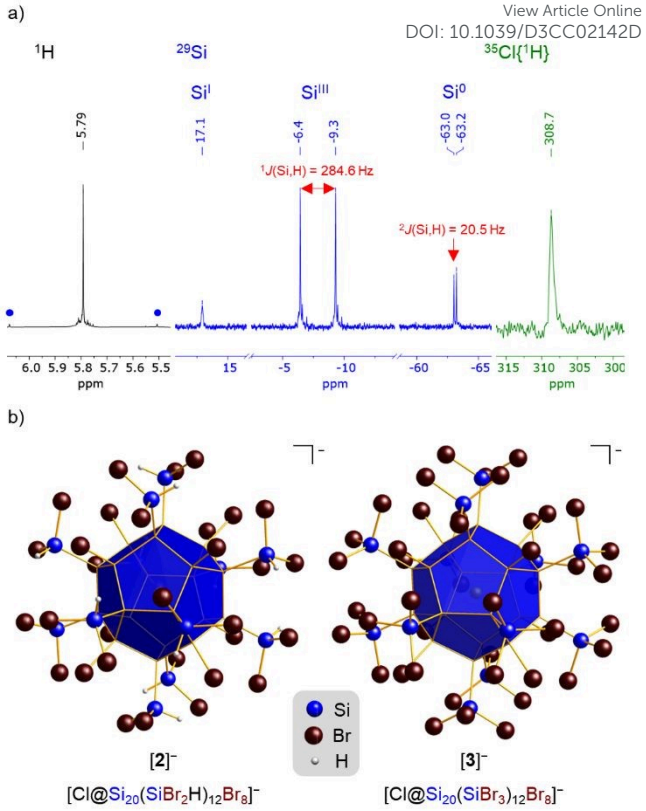

Fig. 2 (a) ^{1}H, ^{29}Si, and ^{35}Cl{^{1}H} NMR spectra of [nBu$_4$N][**2**] (*o*DFB/C_6D_{12} 5:1). In the ^{1}H NMR spectrum, ^{29}Si satellites are marked with blue dots. (b) Crystallographically determined structures of the silafullerane salts [nBu$_4$N][**2**] and [nBu$_4$N][**3**] in the solid state (for clarity, the cations are omitted and only the major occupied sites of the disordered $SiBr_2H$ groups of [**2**]$^-$ are shown).

provides selective access to [nBu$_4$N][Cl@Si$_{20}$(SiBr$_2$H)$_{12}$Br$_8$] ([nBu$_4$N][**2**]), [nBu$_4$N][Cl@Si$_{20}$(SiBr$_3$)$_{12}$Br$_8$] ([nBu$_4$N][**3**]), and [nBu$_4$N][Cl@Si$_{20}$(SiH$_3$)$_{12}$Br$_8$] ([nBu$_4$N][**4**]) showing different degrees of bromination (Scheme 1).

At room temperature, a suspension of [nBu$_4$N][**1**] in *ortho*-difluorobenzene (*o*DFB) reacts with BBr_3 (120 eq.) within 30 min to afford [nBu$_4$N][Cl@Si$_{20}$(SiBr$_2$H)$_{12}$Br$_8$] ([nBu$_4$N][**2**]) in >90% yield. Analogous to [**A**]$^-$, the anion [**2**]$^-$ carries 8 cluster-bonded halogen atoms; in contrast to [**A**]$^-$, [**2**]$^-$ is decorated with 12 $SiBr_2H$ instead of 12 $SiCl_3$ groups. As anticipated, the exhaustively brominated analog of [**A**]$^-$ is apparently too sterically loaded to be accessible under ambient conditions. Pushing the system towards perbrominated [nBu$_4$N][Cl@Si$_{20}$(SiBr$_3$)$_{12}$Br$_8$] ([nBu$_4$N][**3**]) requires the use of 300 eq. of BBr_3, an elevated temperature of 130 °C, and an increased reaction time of 3 d (sealed glass tube). Moreover, a low concentration of ≤5 mmol L^{-1} should be maintained to avoid premature precipitation of poorly soluble products that are almost – but not completely – perbrominated. Taking advantage of the higher reactivity of silyl-bonded compared to cluster-bonded Br atoms, we finally achieved the synthesis of the mixed SiH_3/Br-substituted silafullerane [nBu$_4$N][Cl@Si$_{20}$(SiH$_3$)$_{12}$Br$_8$] ([nBu$_4$N][**4**]) from [nBu$_4$N][**2**] and iBu$_2$AlH (30 eq., *o*DFB/Et$_2$O, room temperature, 16 h). [nBu$_4$N][**4**] was isolated by precipitation from the reaction mixture through addition of *n*-hexane (35% yield). The colorless compounds [nBu$_4$N][**2**]–[nBu$_4$N][**4**] are sensitive toward air, moisture, and tetrahydrofuran (THF).

All NMR spectra were recorded in *o*DFB/C_6D_{12} (5:1 mixtures). In the ^{1}H NMR spectrum, [**2**]$^-$ shows one singlet at 5.79 ppm with ^{29}Si satellites (Fig. 2a; ^1J(H,Si) = 284.6 Hz, cf. HBr$_2$Si–SiBr$_2H$: ^1J(H,Si) = 293.1 Hz[23]); [**3**]$^-$ does no longer give rise to a resonance assignable to Si-bonded H atoms. In the case of [**4**]$^-$, one intense signal at 3.73 ppm (^1J(H,Si) = 203.4 Hz) arises from the chemically equivalent SiH_3 groups (cf. [**1**]$^-$: δ(^{1}H) = 3.47, ^1J(H,Si) = 191.8 Hz[3]). The fact that the SiH_3 nuclei of [**4**]$^-$ are significantly more shielded than the SiHBr$_2$ nuclei of [**2**]$^-$ is consistent with the commonly observed deshielding effect of halogen substituents on geminally positioned protons in mixed hydrido(halogeno)silanes.[23,24] Due to the poor solubility of [nBu$_4$N][**3**], no meaningful ^{29}Si NMR spectra could be recorded. Each of the two anions [**2**]$^-$ and [**4**]$^-$ is characterized by three ^{29}Si NMR signals for its Si^0, Si^I, and Si^{III} centers, which testifies to the postulated average T_h symmetries of the siladodecahedranes in solution and, in turn, to highly selective substitution reactions. In the case of [**2**]$^-$, not only ^1J(H,Si) = 284.6 Hz (d; Si^{III}), but also ^2J(H,Si) = 20.5 Hz (d; Si^0) is resolved (Fig. 2a). All experimentally determined δ(^{29}Si) chemical shifts are in good agreement with the corresponding computed values (Table 1). The endohedral Cl$^-$ ion within each of the cages [**2**]$^-$–[**4**]$^-$ gives rise to one sharp ^{35}Cl NMR resonance. Since ^{35}Cl is a quadrupolar nucleus (I = 3/2),[25] this rarely observed feature requires a near-negligible electric field gradient inside the dodecahedron, which is only fulfilled if the substitution pattern maintains high symmetry. δ(^{35}Cl) is a useful probe of the degree of the Cl$^-$⟶Si$_{20}$ host-guest interaction: the upfield shift of δ(^{35}Cl) along the series [**1**]$^-$⟶[**4**]$^-$⟶[**2**]$^-$⟶[**3**]$^-$ (Table 1) is diagnostic for an increasing Cl$^-$⟶Si$_{20}$ interaction[2] upon increasing the number of electronegative Br atoms in the substituent spheres.

The presence of Si–H bonds in [**2**]$^-$ and [**4**]$^-$ is also indicated by IR-stretching bands at $\tilde{\nu}$(Si–H) = 2177 cm^{-1} (calcd.: 2225 cm^{-1})

Table 1. Experimental (calculated) ^{29}Si and ^{35}Cl NMR-spectroscopic parameters of the silafullerenes [*n*Bu$_4$N][**A**], [*n*Bu$_4$N][**B**], and [*n*Bu$_4$N][**1**]–[*n*Bu$_4$N][**4**] (experimental data and calculated ^{29}Si chemical shift values for [*n*Bu$_4$N][**A**],[1–3] [*n*Bu$_4$N][**B**],[3] and [*n*Bu$_4$N][**1**][3] as previously reported).[a] NMR shifts were calculated at the SO-ZORA-PBE0[27](COSMO(CH$_2$Cl$_2$))[28,29]/ZORA/TZP[30,31]//PBEh-3c[32](SMD(CH$_2$Cl$_2$))[33] level of theory applying ORCA 5.0.3[34–36] for the geometry optimization and AMS2022.101[37] for the NMR shielding calculation. More computational details can be found in the ESI.

Compound	δ(^{29}Si)			δ(^{35}Cl)
	Si^0	Si^I	Si^{III}	
[*n*Bu$_4$N][**A**]	–60.3	31.1	10.3	274.5
	(–63.5)	(31.7)	(15.9)	(278.3)[c]
[*n*Bu$_4$N][**B**]	–73.4	51.5	–97.7	363.7
	(–72.6)	(54.3)	(–98.5)	(360.6)[c]
[*n*Bu$_4$N][**1**]	–58.5	–14.9	–93.7	469.0
	(–58.3)	(–23.9)	(–98.6)	(472.2)[c]
[*n*Bu$_4$N][**2**]	–63.1	17.1	–7.9[b]	308.7
	(–63.6)	(18.6)	(1.8)	(308.8)[c]
[*n*Bu$_4$N][**3**]	n. o.[d]	n. o.[d]	n. o.[d]	271.2
	(–59.8)	(6.7)	(–15.9)	(268.4)[c]
[*n*Bu$_4$N][**4**]	–68.1[e]	35.4[e]	–93.9[e]	372.9
	(–67.1)	(38.5)	(–95.1)	(371.2)[c]

a: NMR spectra were recorded in *o*DFB/C$_6$D$_{12}$ (5:1 mixture) with the exception of the spectra of [*n*Bu$_4$N][**A**] and [*n*Bu$_4$N][**1**], which were measured in THF-d_8.[1,3] b: See Table S2 for NMR-spectroscopic parameters of H/Br-substituted disilanes (H$_{3-n}$Br$_n$Si–*Si*Br$_2$H, *n* = 0–3[23]). c: These values were obtained after scaling according to the following linear equation: δ(^{35}Cl, scaled) = 0.8728 δ(^{35}Cl, calcd) – 7.3179. d: n. o. = not observed. e: The δ(^{29}Si) values of [*n*Bu$_4$N][**4**] were determined by ^{1}H^{29}Si-HSQC and HMBC experiments.

and 2136 cm^{-1} (calcd.: 2180 cm^{-1}),[26] respectively; a corresponding signal is absent in the IR spectrum of [**3**]$^-$. Laser-desorption ionization (LDI) mass spectrometry in the negative-ion mode provided further insight into the composition of our silafullerane products: The molecular-ion peak [M]$^-$ of [**4**]$^-$ was detected with a matching isotope pattern at *m/z* = 1609.82 Da (calcd.: 1609.85 Da), next to the peaks of side products with slightly deviating H/Br distribution. Analogous to [**1**]$^-$,[3] also [**4**]$^-$ undergoes SiH$_2$ elimination under the conditions of mass spectrometry. The molecular masses of [**2**]$^-$ (3503.67 Da) and [**3**]$^-$ (4450.59 Da) are so high that the limit of our matrix-free LDI(–)-MS approach is reached,[38] but peaks of characteristic fragmentation products could still be detected: In the case of [**2**]$^-$ ([Cl@Si$_{32}$H$_{12}$Br$_{32}$]$^-$), the peak of [Cl@Si$_{30}$H$_{11}$Br$_{29}$]$^-$ (*m/z* = 3203.85 Da; calcd.: 3203.96 Da) is particularly noteworthy as it indicates elimination both of SiBr$_2$ and SiHBr fragments from SiBr$_2$H groups of the silafullerane. Products of stepwise SiBr$_2$ elimination were also detected in the LDI(–) MS of [*n*Bu$_4$N][**3**]. Among them, the [M–6×SiBr$_2$]$^-$ peak (*m/z* = 3323.64 Da; calcd.: 3323.72 Da) corresponds to the heaviest fragment of [**3**]$^-$, which could be unambiguously assigned on its isotope pattern.

Crystals of [*n*Bu$_4$N][**2**] and [*n*Bu$_4$N][**3**] suitable for X-ray analysis were obtained from *o*DFB solutions at –30 °C and 130 °C→room temperature, respectively (Fig. 2b; cf. the ESI for details). In both structures, the silafullerane anions are located on inversion centers. In the structure of [*n*Bu$_4$N][**2**], three of the six crystallographically independent SiBr$_2$H groups are disordered by rotation about the Si–Si bonds to the cluster core; the sums of the respective occupation factors agree with a number of 2 Br atoms per silyl group in all cases. The presence of 44 Br substituents in [*n*Bu$_4$N][**3**] was confirmed using data from a synchrotron measurement. The Si–Si bond lengths in partially brominated [*n*Bu$_4$N][**2**] (2.324(5)–2.374(5) Å) and perbrominated [*n*Bu$_4$N][**3**] (2.329(2)–2.376(2) Å) are similar to each other, but slightly larger than those in perchlorinated [*n*Bu$_4$N][**A**] (2.295(3)–2.360(2) Å;[1] values, differentiated by bond type, are given in the ESI). In [*n*Bu$_4$N][**2**], the vicinal SiBr$_2$H groups are mainly oriented such that pairs of H···Br contacts are found between them (to give six-membered -[Si–H···Br–Si–H···Br]- rings). In [*n*Bu$_4$N][**3**], 12 short Br···Br contacts (3.7022(12)–3.7823(15) Å) that are close to the sum of the van der Waals radii of two Br atoms (3.70 Å[39]) cannot be avoided between adjacent SiBr$_3$ substituents. As a result, increased Si^{III}···Si^{III} distances and Si^{III}–Si^0–Si^0 angles are found within the silyl-group pairs of [*n*Bu$_4$N][**3**] vs. [*n*Bu$_4$N][**2**] (Si^{III}···Si^{III} = 4.578(3)–4.617(3) vs. 4.260(6)–4.423(6) Å, Si^{III}–Si^0–Si^0 = 116.31(9)–120.39(8) vs. 112.89(19)–118.30(18)°). Furthermore, the Br···Br distances between silyl- and cluster-bonded Br atoms in [*n*Bu$_4$N][**3**] (3.5866(11)–3.933(1) Å) are shorter than the analogous distances in [*n*Bu$_4$N][**2**] (3.791(1)–4.113(3) Å). These trends, which are also evident when comparing the corresponding calculated structures (cf. the ESI), suggest higher steric hindrance within the substituent sphere of the perbrominated silafullerane [*n*Bu$_4$N][**3**] relative to partially brominated [*n*Bu$_4$N][**2**].

The silafullerane anion [Cl@Si$_{20}$(SiH$_3$)$_{12}$H$_8$]$^-$ ([**1**]$^-$) stands out for its 44 functionalizable groups and therefore represents a potential entry point for a rich follow-up chemistry. However, this is only valid under the condition that one can derivatize either all or a pre-defined subset of the Si–H bonds. We have now succeeded in the perbromination of [**1**]$^-$ to give [**3**]$^-$, albeit only at high temperatures (130 °C, 300 eq. BBr$_3$) and on a small scale. In situ monitoring of the reaction progress revealed that the harsh reaction conditions are mainly required to enforce the last few H/Br-exchange steps and the associated massive build-up of steric repulsion. Based on these findings, it was possible to optimize the reaction protocol in a way that allows the synthesis of regioselectively brominated [Cl@Si$_{20}$(SiBr$_2$H)$_{12}$Br$_8$]$^-$ in >90% yield ([**2**]$^-$; room temperature, 120 eq. BBr$_3$, 30 min). The subsequent hydrogenation of [**2**]$^-$ with *i*Bu$_2$AlH straightforwardly furnishes [Cl@Si$_{20}$(SiH$_3$)$_{12}$Br$_8$]$^-$ ([**4**]$^-$). Considering that Si–H and Si–Br bonds exhibit largely orthogonal reactivity (e.g., hydrosilylation vs. nucleophilic substitution), the stage is now set for the facile regioselective introduction of more sophisticated functional groups.

M.W. thanks the Deutsche Forschungsgemeinschaft (DFG) for financial support (grant no. 506550642). S.G. and M.Bu. gratefully acknowledge financial support by the Max Planck Society through the Max Planck fellow program. M.Ba. wishes to thank the Fonds der Chemischen Industrie (FCI) for a Kekulé Ph.D. grant. The authors are grateful to Evonik Operations GmbH, Rheinfelden (Germany), for the generous donation of Si$_2$Cl$_6$. Parts of this research (project I-20220865) were carried out at PETRA III at DESY, a member of the Helmholtz Association (HGF). A.V. and M.Ba. thank Dr. Leila Noohinejad, Dr. Martin Tolkiehn and Dr. Eugenia Peresypkina for their assistance regarding the use of the beamline P24. A.V. thanks Dr. Matthias

Meyer (Rigaku Oxford Diffraction) for his precious help with the implementation of the *CrysAlisPro* software for the synchrotron and STOE IPDS II diffraction data. M.W. and M.Ba. wish to thank Matthias Brandl for his continuing support regarding the measurement of LDI mass spectra.

Conflicts of interest

There are no conflicts to declare.

Notes and references

1 J. Tillmann, J. H. Wender, U. Bahr, M. Bolte, H.-W. Lerner, M. C. Holthausen and M. Wagner, *Angew. Chem., Int. Ed.*, 2015, **54**, 5429–5433.
2 M. Bamberg, M. Bursch, A. Hansen, M. Brandl, G. Sentis, L. Kunze, M. Bolte, H.-W. Lerner, S. Grimme and M. Wagner, *J. Am. Chem. Soc.*, 2021, **143**, 10865–10871.
3 M. Bamberg, T. Gasevic, M. Bolte, A. Virovets, H.-W. Lerner, S. Grimme, M. Bursch and M. Wagner, *J. Am. Chem. Soc.*, 2023, DOI: 10.1021/jacs.3c03270.
4 J. Teichmann and M. Wagner, *Chem. Commun.*, 2018, **54**, 1397–1412.
5 S. Nagase, *Acc. Chem. Res.*, 1995, **28**, 469–476.
6 F. Pichierri, V. Kumar and Y. Kawazoe, *Chem. Phys. Lett.*, 2005, **406**, 341–344.
7 F. Marsusi and M. Qasemnazhand, *Nanotechnology*, 2016, **27**, 275704.
8 D. S. De, B. Schaefer, B. von Issendorff and S. Goedecker, *Phys. Rev. B*, 2020, **101**, 214303.
9 N. Wiberg, C. M. M. Finger and K. Polborn, *Angew. Chem., Int. Ed. Engl.*, 1993, **32**, 1054–1056.
10 M. Ichinohe, M. Toyoshima, R. Kinjo and A. Sekiguchi, *J. Am. Chem. Soc.*, 2003, **125**, 13328–13329.
11 H. Matsumoto, K. Higuchi, Y. Hoshino, H. Koike, Y. Naoi and Y. Nagai, *J. Chem. Soc., Chem. Commun.*, 1988, **17**, 1083–1084.
12 K. Furukawa, M. Fujino and N. Matsumoto, *Appl. Phys. Lett.*, 1992, **60**, 2744–2745.
13 J. Fischer, J. Baumgartner and C. Marschner, *Science*, 2005, **310**, 825.
14 T. C. Siu, M. Imex Aguirre Cardenas, J. Seo, K. Boctor, M. G. Shimono, I. T. Tran, V. Carta and T. A. Su, *Angew. Chem., Int. Ed.*, 2022, **61**, e202206877.
15 D. Scheschkewitz, *Angew. Chem., Int. Ed.*, 2005, **44**, 2954–2956.
16 T. Iwamoto, N. Akasaka and S. Ishida, *Nat. Commun.*, 2014, **5**, 5353.
17 J. Keuter, C. Schwermann, A. Hepp, K. Bergander, J. Droste, M. R. Hansen, N. L. Doltsinis, C. Mück-Lichtenfeld and F. Lips, *Chem. Sci.*, 2020, **11**, 5895–5901.
18 J. Helmer, A. Hepp and F. Lips, *Dalton Trans.*, 2022, **51**, 3254–3262.
19 S. Scharfe, F. Kraus, S. Stegmaier, A. Schier and T. F. Fässler, *Angew. Chem., Int. Ed.*, 2011, **50**, 3630–3670.
20 M. Waibel, F. Kraus, S. Scharfe, B. Wahl and T. F. Fässler, *Angew. Chem., Int. Ed.*, 2010, **49**, 6611–6615.
21 M. Neumeier, F. Fendt, S. Gärtner, C. Koch, T. Gärtner, N. Korber and R. M. Gschwind, *Angew. Chem., Int. Ed.*, 2013, **52**, 4483–4486.
22 Y. Heider and D. Scheschkewitz, *Chem. Rev.*, 2021, **121**, 9674–9718.
23 K. Hassler and G. Bauer, *J. Organomet. Chem.*, 1993, **460**, 149–153.
24 H. Söllradl and E. Hengge, *J. Organomet. Chem.*, 1983, **243**, 257–269.
25 J. W. Akitt, in *Multinuclear NMR*, ed. J. Mason, Springer, Boston, 1987, pp. 447–461.
View Article Online DOI: 10.1039/D3CC02142D
26 IR stretching bands were calculated at the PBEh-3c(SMD(CH_2Cl_2))//PBEh-3c(SMD(CH_2Cl_2)) level of theory in ORCA 5.0.3.
27 C. Adamo and V. Barone, *J. Chem. Phys.*, 1999, **110**, 6158–6170.
28 A. Klamt and G. Schüürmann, *J. Chem. Soc., Perkin Trans. 2*, 1993, 799–805.
29 C. P. Pye, T. Ziegler, E. van Lenthe and J. N. Louwen, *Can. J. Chem*., 2009, **87**, 790–797.
30 E. van Lenthe, E. J. Baerends and J. G. Snijders, *J. Chem. Phys.*, 1994, **101**, 9783–9792.
31 E. van Lenthe and E. J. Baerends, *J. Comput. Chem.*, 2003, **24**, 1142–1156.
32 S. Grimme, J. G. Brandenburg, C. Bannwarth and A. Hansen, *J. Chem. Phys.*, 2015, **143**, 054107.
33 A. V. Marenich, C. J. Cramer and D. G. Truhlar, *J. Phys. Chem. B*, 2009, **113**, 6378–6396.
34 F. Neese, *Wiley Interdiscip. Rev. Comput. Mol. Sci.*, 2012, **2**, 73–78.
35 F. Neese, F. Wennmohs, U. Becker and C. Riplinger, *J. Chem. Phys.*, 2020, **152**, 224108.
36 F. Neese, *Wiley Interdiscip. Rev. Comput. Mol. Sci*, 2022, **12**, e1606.
37 R. Rüger, M. Franchini, T. Trnka, A. Yakovlev, E. van Lente, P. Philipsen, T. van Vuren, B. Klumpers and T. Soini, ADF 2022.1, SCM, Theoretical Chemistry, Vrije Universiteit, Amsterdam, The Netherlands, http://www.scm.com, 2022 (accessed 2023-04-26).
38 Matrix materials commonly used in MALDI-MS are chemically incompatible with the sensitive silafullerane anions.
39 A. Bondi, *J. Phys. Chem.*, 1964, **68**, 441–451.